

SPECTROSCOPY OF ATOMS
AND MOLECULES

Reduced Doppler Absorption Profile in Atomic and Molecular Beams

N. N. Bezuglov^a, M. Yu. Zakharov^a, A. N. Klyucharev^a, A. A. Matveev^a,
K. Michulis^b, É. Saks^b, I. Sydoryk^b, and A. Ékers^b

^a Fock Research Institute of Physics, St. Petersburg State University, Peterhof, St. Petersburg, 198504 Russia

^b Institute of Atomic Physics and Spectroscopy, University of Latvia, LV-1586 Riga, Latvia

e-mail: andrei.matveev@inbox.ru

Received December 28, 2006

Abstract—The formation of the Doppler absorption profile $P(\nu)$ upon optical excitation of particles in the volume of effusion or gas-dynamic atomic and molecular beams by laser light propagating in a direction orthogonal (reduced) to the beam axis is considered. The analytical expressions for $P(\nu)$ are obtained for different types of beams and the specific features of the reduced absorption profile are studied as functions of the beam parameters. The function $P(\nu)$ is shown to be considerably different from the standard Gaussian shape. It is demonstrated that the calculated absorption spectrum at the frequencies of the sodium resonance lines $D_{1,2}$ agrees well with experiment.

PACS numbers: 32.70.-n

DOI: 10.1134/S0030400X07060033

INTRODUCTION

The atomic and molecular beams (ABs) are traditionally used in spectroscopic investigations to obtain low thermal (subthermal) velocities v_{ST} of relative motion of particles. In particular, it is well known [1, 2] that the characteristic velocity v_{ST} in an effusion beam (EB) is threefold lower than the average thermal velocity v_T of particles of an effusion source. This decreases the average collision energy of the beam particles by almost an order of magnitude ($3^2 = 9$). Another practically important feature of ABs consists in rather narrow absorption profiles owing to the unidirectional propagation of an AB along its axis (the z axis in Fig. 1a). The

line narrowing increases the efficiency of optical excitation of ABs, as a result of which the beam volume may have a noticeable optical thickness for the resonance radiation even at comparatively low concentrations of normal atoms ($\sim 10^{11} \text{ cm}^{-3}$) [3]. The maximum narrowing of the spectral lines is realized when the photon beam is orthogonal to the AB direction. In this case, for a perfectly collimated AB, the Doppler broadening is absent and the line profile is determined by the natural broadening. A finite nonzero collimation angle φ gives rise to the reduced Doppler width $\Delta\nu_D \approx v_T/\lambda \sin\varphi$, where λ is the wavelength of the resonance line and v_T is the characteristic velocity of the unidirectional motion of the AB particles. For typical experi-

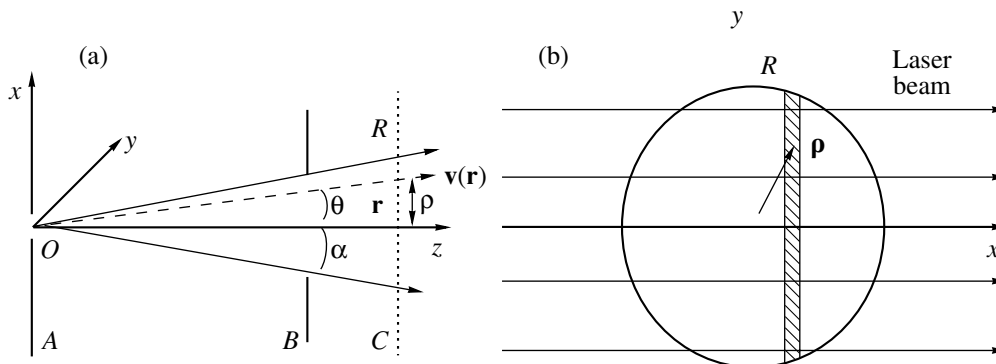


Fig. 1. (a) Geometry of the atomic beam. (A) effusion source, (B) collimating slit, and (C) excitation zone. (b) Excitation plane $C\{x, y\}$. The incident laser radiation is orthogonal to the beam axis z .

mental parameters ($\lambda \approx 5890 \text{ \AA}$, $v_T \sim 400 \text{ m/s}$, and $\varphi \sim 1^\circ$), we have $\Delta v_D = 12 \text{ MHz}$, which considerably exceeds the natural width $\Delta v_{\text{nat}} = 1/(\tau_{\text{nat}} 4\pi) = 4.9 \text{ MHz}$ of the sodium resonance line. It follows from this that, in particular, the reduced Doppler profile $P_D(v)$ is formed by different regions of the beam with different Doppler shifts. In this paper, we calculate the profile $P_D(v)$ for two types of ABs and demonstrate that it differs from the Gaussian profile, which is traditionally used to describe Doppler profiles.

EXPERIMENTAL SETUP AND AB PARAMETERS

The schematic of atomic beams is shown in Fig. 1a. Particles (atoms or molecules) of the beam are created in the vaporous phase by heating in an effusion source A at the temperature T and directed to the reaction zone C through an aperture O . A collimator B cuts out from the angular distribution of particles a narrow solid angle with the opening φ (the collimation angle), which ensures a necessary degree of unidirectionality of beam particles. In this study, we will use some simplifying assumptions, typical for practical schemes of spectroscopic experiments. (i) The size of the aperture O is negligibly small in comparison with the other characteristic lengths of the problem (for example, the radius of the collimating aperture and the radius R of the excitation zone). (ii) This allows us to assume that the trajectories of particles, passing through a point \mathbf{r} in the excitation zone, are unidirectional, i.e., we can unambiguously relate the directions of their velocities $\mathbf{v}(\mathbf{r})$ with the direction \mathbf{r} : $\mathbf{v}(\mathbf{r}) = |\mathbf{v}(\mathbf{r})|\mathbf{r}/|\mathbf{r}|$. (iii) Projecting this equality onto the excitation plane C , we can obtain the important relation

$$\mathbf{v}_\perp(\mathbf{r}) = v\theta\mathbf{p}/|\mathbf{p}| = \varphi v\mathbf{p}/R, \quad v \equiv |\mathbf{v}(\mathbf{r})| \quad (1)$$

between the projection \mathbf{v}_\perp of the particle velocity onto the excitation plane and the observation point $\mathbf{p} = \{x, y\}$ in the plane C (Fig. 1b). Obviously, formula (1) is valid if the collimation angle φ is assumed to be small. (iv) The thickness of the excitation zone is taken to be negligibly small in comparison with the distance to the effusion source, which allows us to assume that the spatial distribution of AB particles is homogeneous.

These assumptions completely characterize the distribution of particles over velocity directions. The normalized distribution $F(v)$ over the absolute velocity v is determined by the Maxwell function [4–6]

$$F_e(v) = \frac{4v^2}{\sqrt{\pi}v_T^3} \exp\left(-\frac{v^2}{v_T^2}\right), \quad (2)$$

where $v_T = \sqrt{\frac{2kT}{m}}$, for EBs or by the function

$$F_{\text{gd}}(v) = \frac{v^2}{\sqrt{\pi}v_f^2 v_T} \exp\left(-\frac{(v - v_f)^2}{v_T^2}\right) \quad (3)$$

for gas-dynamic beams (GDBs) [4, 7]. The quantity v_T (2) for EBs coincides with the thermal velocity of particles in an effusion source maintained at a temperature T and has the order of $\sim 400 \text{ m/s}$ for sodium atoms. In the case of a GDB, v_T is determined by the process of expansion (cooling) of the gas jet in the nozzle (typically, $v_T \sim 200 \text{ m/s}$). In this case, the characteristic velocity of motion of GDB particles is the mass velocity $v_f \sim 1000 \text{ m/s}$ [7].

THE INTEGRAL REPRESENTATION FOR A REDUCED DOPPLER PROFILE

Let us consider the excitation of an AB by a monochromatic laser beam directed perpendicular to the AB axis (the z axis) along the x axis (Fig. 1b). Since the Doppler frequency shift Δv depends on the angle between the direction of photons and AB particles, we will study the distribution of the velocity projection \mathbf{v}_\perp (1) onto the excitation plane C . The quantity Δv is directly related to the x component $\mathbf{v}_{\perp, x} \equiv v_x$ as

$$\Delta v = \frac{v_x}{\lambda} = \frac{\varphi v x}{\lambda R} \quad (4)$$

and, as is seen, has a complicated dependence on the spatial position of an AB particle (the x coordinate) and on its velocity modulus v . By definition, the reduced Doppler absorption profile $\tilde{P}(\Delta v)$ should be sought from the relative number (probability) $P(\Delta v)d\Delta v$ of particles in the excitation zone, whose Doppler shift falls into the frequency region $(\Delta v, \Delta v + d\Delta v)$. The calculation of $P(\Delta v)$ according to (4) is equivalent to the determination of the probability $\tilde{P}(v_x)$ of finding a particle whose x component of \mathbf{v}_\perp is v_x : $P(\Delta v) = \lambda \tilde{P}(\lambda \Delta v)$.

We will reduce the problem of finding of $\tilde{P}(v_x)$ to the calculation of average values, i.e., we will consider a function $f(\tau)$ that depends only on the x component of the particle velocity, $\tau = v_x$. If we succeed in finding the average value of f

$$\langle f \rangle \equiv \int_{-\infty}^{\infty} d\tau \tilde{P}(\tau) f(\tau) \quad (5)$$

for AB particles in the reaction zone for a random f , we will be able to find the distribution $\tilde{P}(v_x)$ for $f_{v_x}(\tau) = \delta(\tau - v_x)$ from (5) (where δ is the one-dimensional Dirac δ function). The finding of $\langle f \rangle$ reduces to two simple operations: first, we should average f inside the excitation zone (i.e., in the area πR^2 on the plane C)

and, second, to average it over the velocity distribution $F(v)$:

$$\langle f \rangle = 1/(\pi R^2) \iint_C dx dy \int_0^\infty dv F(v) f(\varphi vx/R). \quad (6)$$

By virtue of the assumption of spatial homogeneity of AB particles, the double integration over the plane C (i.e., when $x^2 + y^2 \leq R^2$) enters with a constant weight equal to the reciprocal area of the plane. Substituting the function f_{v_x} defined above into (6), we come to the representation

$$\begin{aligned} \tilde{P}(v_x) &= 2/(\pi R^2) \int_{-R}^R dx \sqrt{R^2 - x^2} \\ &\times \int_0^\infty dv F(v) \delta(v_x - \varphi vx/R), \end{aligned} \quad (7)$$

which, together with the relation $P(\Delta v) = \lambda \tilde{P}(\lambda \Delta v)$, gives the sought formula for calculating the profile $P(\Delta v)$:

$$P(\Delta v) = \frac{2\lambda}{\pi\varphi} \int_{|\lambda\Delta v|/\varphi}^\infty \frac{dv}{v^2} F(v) \sqrt{v^2 - \frac{\lambda^2 \Delta v^2}{\varphi^2}}. \quad (8)$$

THE PROPERTIES AND SPECIFIC FEATURES OF THE PROFILE $P(\Delta v)$

Relationship (8) is an exact integral representation for the reduced Doppler profile in the case of a random velocity distribution $F(v)$ of AB particles. It allows a simplified description for two types of beams, EBs and GDBs, which will be considered separately.

An Effusion Beam

In this case, the distribution $F(v)$ has form (2) and the corresponding Doppler profile is equal to

$$P_e(\Delta v) = \frac{8\Delta v^2}{\pi^{3/2} \Delta v_{De}^3} \Phi_e\left(\frac{\Delta v}{\Delta v_{De}}\right), \quad (9)$$

where $\Delta v_{De} = \varphi v_T / \lambda$

$$\Phi_e(\xi) = \int_1^\infty d\tau \sqrt{\tau^2 - 1} \exp(-\xi^2 \tau^2). \quad (10)$$

Relation (9) includes the function Φ_e , which depends on one variable. The parameter Δv_{De} obviously represents the characteristic Doppler width for a reduced profile P_e . The analytical properties of the function P_e

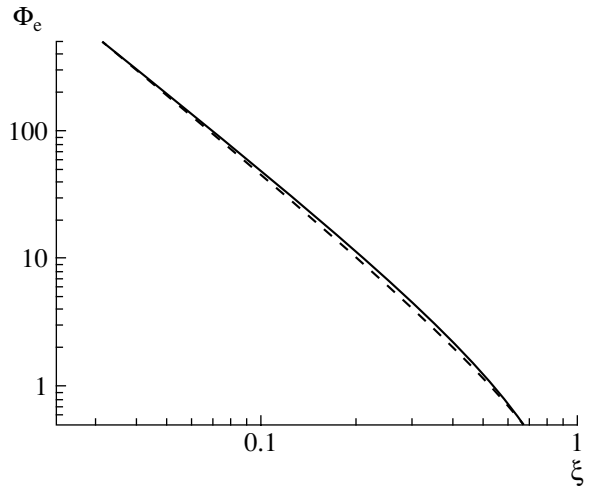


Fig. 2. Comparison of the function Φ_e (10) and its approximation $\tilde{\Phi}_e$ (13).

are analyzed in the Appendix, which, in particular, gives the asymptotics of Φ_e ,

$$\Phi_e(\xi) \xrightarrow{\xi \rightarrow 0} 1/(2\xi^2), \quad (11)$$

$$\Phi_e(\xi) \xrightarrow{\xi \rightarrow \infty} \frac{\sqrt{\pi}}{4} \exp(-\xi^2)/\xi^3. \quad (12)$$

Based on these asymptotics, it is easy to construct a simplest approximation of $\tilde{\Phi}_e$ with properties (11) and (12) in the region of large and small values of the argument ξ ,

$$\tilde{\Phi}_e(\xi) = 1/(2\xi^2) \frac{\sqrt{\pi}}{\sqrt{\pi} + 2|\xi| \exp(\xi^2)}. \quad (13)$$

Figure 2 shows the plots of both functions, Φ_e (the solid curve) and $\tilde{\Phi}_e$ (the dashed curve). It is seen that $\tilde{\Phi}_e$ approximates Φ_e with an error not exceeding 15% and, hence, the profile P_e can be approximated with the same level of accuracy as

$$\begin{aligned} P_e(\Delta v) \\ \approx \frac{4}{\pi \Delta v_{De} \sqrt{\pi} + 2|\Delta v|/\Delta v_{De} \exp(\Delta v^2/\Delta v_{De}^2)}. \end{aligned} \quad (14)$$

Formula (14) considerably differs from the standard Doppler shape but, nevertheless, predicts typical exponential slopes in the line wings.

A Gas-Dynamic Beam

The velocity distribution $F(v)$ for GDBs is described by relation (3), the substitution of which into

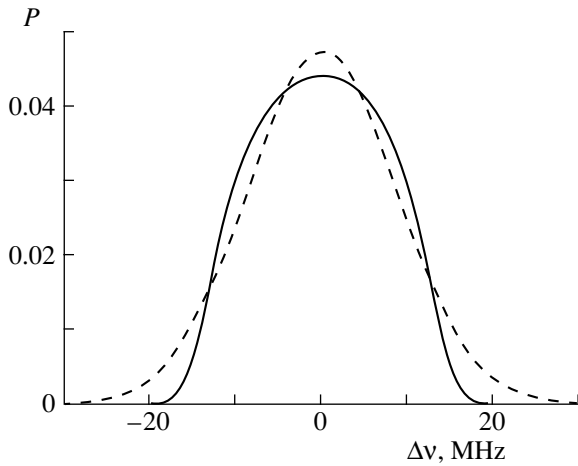


Fig. 3. Function $P_{\text{gd}}(\Delta\nu)$ (solid curve) and its Gaussian approximation (dashed curve).

formula (8) leads to the following form of the reduced Doppler profile $P_{\text{gd}}(\Delta\nu)$:

$$P_{\text{gd}}(\Delta\nu) = \frac{2\Lambda}{\pi^{3/2}} \frac{\Delta\nu^2}{\Delta\nu_{\text{Dgd}}^3} \int_0^\infty d\tau \sqrt{\tau^2 - 1} \times \exp[-\Lambda^2 (\tau|\Delta\nu|/\Delta\nu_{\text{Dgd}} - 1)^2], \quad (15)$$

where

$$\Delta\nu_{\text{Dgd}} = \varphi v_f / \lambda; \quad \Lambda = v_f / v_T. \quad (16)$$

Here, the value $\Delta\nu_{\text{Dgd}}$ plays the role of a characteristic reduced Doppler width. Note the appearance in formula (15) of a large parameter Λ , whose value for typical conditions of experiments with GDBs is $\Lambda \approx 5$. Since $\Delta\nu_{\text{Dgd}} = \Lambda \Delta\nu_{\text{De}}$, the reduced Doppler profile for EBs is five times narrower than for GDBs. In this paper, we do not analyze the analytical properties of the function $P_{\text{gd}}(\Delta\nu)$ (15) and its possible approximations (this will be done elsewhere) and restrict ourselves to the illustration of the form of P_{gd} for the typical values $\Lambda = 5$ and $\Delta\nu_{\text{Dgd}} = 14$ MHz (Fig. 3). The dashed line in Fig. 3 shows the optimal fitting (obtained by the least squares method) of the standard Gaussian function to $P_{\text{gd}}(\Delta\nu)$. It is clearly seen that the real behavior of P_{gd} differs from the characteristic exponential shape of Doppler profiles.

COMPARISON WITH EXPERIMENTAL DATA

The experimental data (points) on the excitation of the $D_{1,2}$ resonance lines of sodium are presented in Figs. 4 and 5. A gas-dynamic beam of Na atoms was irradiated by a relatively weak monochromatic laser beam (1.5 mm in diameter) in the direction orthogonal to the GDB axis. The frequency-integrated fluores-

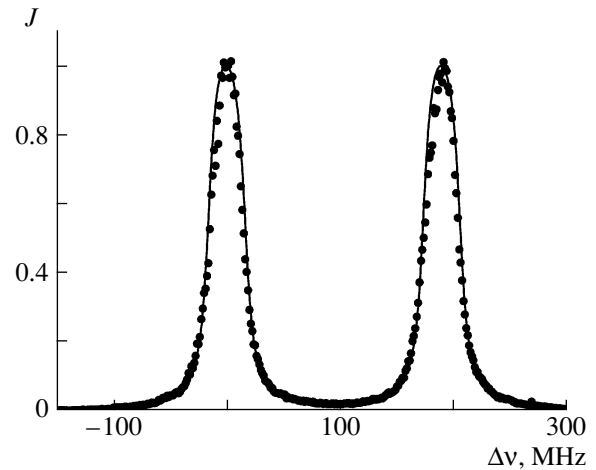


Fig. 4. Experimental (points) and theoretical (solid curve) absorption profiles for the D_1 line of Na in a gas-dynamic beam at $v_f = 1340$ m/s.

cence signal J was recorded at an angle of 45° to the GDB axis. The dependence of J on the laser frequency ν determined the experimental absorption spectrum. The collimation angle was $\varphi = 0.43^\circ$. The experiment for the D_1 line ($\lambda = 589.593$ nm) (Fig. 4) was performed at the mass velocity $v_f = 1340$ m/s, which corresponds to $\Delta\nu_{\text{Dgd}} = 16.9$ MHz. In the case of the D_2 line ($\lambda = 588.996$ nm) (Fig. 5), the mass velocity was $v_f = 1060$ m/s and, correspondingly, $\Delta\nu_{\text{Dgd}} = 13.3$ MHz.

The fluorescence spectra $J(\nu)$ shown in Figs. 4 and 5 correspond to the transitions from the upper HFS sublevel $F = 2$ of the ground $3s_{1/2}$ state. The fluorescence at the frequencies of the D_1 line has two peaks corresponding to the resonance absorption of light upon

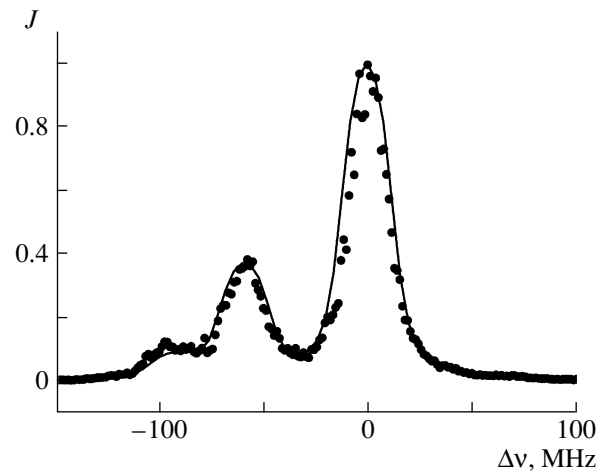


Fig. 5. Experimental (points) and theoretical (solid curve) absorption profiles for the D_2 line of Na in a gas-dynamic beam at $v_f = 1060$ m/s.

transitions $3s_{1/2}(F=2) \rightarrow 3p_{1/2}(F'=1, 2)$. Since the oscillator strengths of these transitions coincide with each other [8], the peaks have equivalent heights. The three peaks of the signal $J(\nu)$ for the D_2 line correspond to the transitions $3s_{1/2}(F=2) \rightarrow 3p_{3/2}(F'=1, 2, 3)$. The ratio of their heights, 1 : 5 : 14, is determined by the ratio of corresponding oscillator strengths [8].

The resonance level $3p_{3/2}$ has a rather short lifetime equal to 16.2 ns and a natural width $\Delta\nu_{\text{nat}} = 4.9$ MHz. The resulting absorption profile $P_{\Sigma}(\Delta\nu)$ is a convolution of the reduced Doppler P_{gd} (15) and Lorentz P_L profiles:

$$P_{\Sigma}(\Delta\nu) = \int_{-\infty}^{\infty} d\eta P_{\text{gd}}(\eta) P_L(\Delta\nu - \eta), \quad (17)$$

$$P_L(\Delta\nu) = \frac{\Delta\nu_{\text{nat}}}{\pi} \frac{1}{\Delta\nu^2 + \Delta\nu_{\text{nat}}^2}.$$

The fluorescence intensity J in the absence of saturation of the optical transition is proportional to P_{Σ} .

The profiles $P_{\Sigma}(\Delta\nu)$, calculated using relations (15)–(17) taking into account the relative line strengths, are shown in Figs. 4 and 5 by solid curves. One can see good agreement between the theoretical and experimental data (points).

CONCLUSIONS

The rate constants of the processes of radiative kinetics are determined to a large extent by the parameters of the experimental setup and strongly depend on the broadening mechanisms of the absorption and emission profiles. For example, under conditions of laser manipulation of quantum states of atoms (molecules) in a gas-dynamic (effusion) beam [7], the ratio of the fluorescence peaks changes with the width of the Doppler absorption profile. This distorts the useful information about the characteristics of excited states, which can be obtained by measuring the corresponding profiles [7]. In this paper, we presented the analytical expressions for the reduced absorption profile formed as a result of different Doppler frequency shift in different spatial points of a light beam. The fluorescence spectra calculated taking into account the obtained expressions for the Doppler profile agree well with experimental data.

APPENDIX

Since we have to study the asymptotic properties of the function Φ_e (10) in different ranges of the argument ξ by different methods, we will derive formulas (11) and (12) in two steps.

Expansion into a Taylor series at small ξ . To analyze the function $\Phi_e(\xi)$, it is very convenient to use the

following Mellin transform [2] of an exponential function:

$$\exp(-x) = \int_{\Pi} \frac{ds}{2\pi i} \Gamma(-s) x^s. \quad (A.1)$$

The integration contour Π in the complex plane of the variable s goes to $-i\infty$ and $+i\infty$ so that integer singular points $s_i = 0, 1, 2, \dots$ of the Euler gamma function $\Gamma(-s)$ [9] are always to the right. The orientation of Π is determined by the direction from $-i\infty$ to $+i\infty$. Representation (A.1) is easily checked by expanding the right- and left-hand sides of (A.1) into the Taylor series in terms of powers of x . The substitution of (A.1) into formula (10) transforms it to the form

$$\Phi_e(\xi) = \int_{\Pi} \frac{ds}{2\pi i} \Gamma(-s) \xi^{2s} \int_1^{\infty} d\tau \tau^{2s} \sqrt{\tau^2 - 1}. \quad (A.2)$$

The second integration over the variable τ reduces to the standard form for combinations of three gamma functions [9], so that (A.2) transforms to

$$\Phi_e(\xi) = -\frac{\sqrt{\pi}}{4} \int_{\Pi} \frac{ds}{2\pi i} \frac{\Gamma(-s) \Gamma(0.5 + s) \cos \pi s}{\Gamma(2 + s) \sin \pi s} \xi^{2s}. \quad (A.3)$$

The integrand is an analytical function of the variable s with the simple singular point (of the first order) $s = -1$ and the integer points $s = 0, 1, 2, \dots$ of the second order. Using the theory of residues, we can easily find the sought Taylor expansion of $\Phi_e(\xi)$ (10) by removing the contour Π from the left half-plane ($\text{Re } s < -1$) to the right half-plane ($\text{Re } s \rightarrow +\infty$) of the variable s ,

$$\Phi_e(\xi) = \frac{1}{2\xi^2} + \sum_{n=0}^{\infty} \frac{(-\xi^2)^n \Gamma(0.5 + n)}{4\sqrt{\pi} n!(n+1)!} \times \left[2\ln(x) + \Psi(0.5 + n) - 2\Psi(1 + n) - \frac{1}{1+n} \right]. \quad (A.4)$$

Here, $\Psi(s)$ is a logarithmic derivative of the Γ function [9].

Asymptotic in the region of large ξ . A slight transformation of integral (10) to the equivalent form

$$\Phi_e(\xi) = \frac{\exp(-\xi^2)}{2} \int_0^{\infty} d\tau \frac{\sqrt{\tau}}{\sqrt{1+\tau}} \exp(-\xi^2 \tau) \quad (A.5)$$

allows us to use the saddle-point method [10] to calculate (A.5) for $\xi \rightarrow +\infty$. In this case, the main contribution to the integral is made by the region of small τ and the sought asymptotic expression is found immediately after expanding the function $(1 + \tau)^{-0.5}$ into the Taylor series:

$$(1 + \tau)^{-0.5} = \sum_{n=0}^{\infty} (-\tau)^n \frac{\Gamma(0.5 + n)}{\sqrt{\pi} n!}; \quad (A.6)$$

$$\Phi_e(\xi) = \frac{\exp(-\xi^2)}{2|\xi|^3} \sum_{n=0}^{\infty} \frac{1}{(-\xi^2)^n} \frac{\Gamma(1.5+n)\Gamma(0.5+n)}{\sqrt{\pi}n!}. \quad (\text{A.7})$$

Relations (11) and (12) contain the first main terms of expansions (A.4) and (A.7), respectively.

ACKNOWLEDGMENTS

This study was supported by the Russian Foundation for Basic Research, project no. 05-03-33252, by the European Program EU FP6 Project LAMOL (EU contract MTKD-CT-2004-014228), and by an NATO grant EAP.RIG.981.378.

REFERENCES

1. V. S. Troitskiĭ, Zh. Éksp. Teor. Fiz. **41**, 389 (1961) [Sov. Phys. JETP **14**, 281 (1962)].
2. A. N. Klyucharev and N. N. Bezuglov, *Processes Excitation and Ionization of Atoms upon Light Absorption* (Leningr. Gos. Univ., Leningrad, 1983) [in Russian].
3. N. N. Bezuglov, A. Ekers, O. Kaufmann, et al., J. Chem. Phys. **119** (1), 7094 (2003).
4. V. B. Leonas, Usp. Fiz. Nauk **127** (2), 319 (1979) [Sov. Phys. Usp. **22** (2), 109 (1979)].
5. N. N. Bezuglov, A. N. Klucharev, and V. A. Sheverev, J. Phys. B **20**, 2495 (1987).
6. K. Miculis, I. I. Beterov, N. N. Bezuglov, et al., J. Phys. B **38**, 1811 (2005).
7. R. Garcia-Fernandez, A. Ekers, J. Klavins, et al., Phys. Rev. A **71**, 023401 (2005).
8. I. I. Sobel'man, *Introduction to the Theory of Atomic Spectra* (Fizmatgiz, Moscow, 1963) [in Russian].
9. I. S. Gradshteĭn and I. M. Ryzhik, *Tables of Integrals, Series, and Products*, 4th ed. (Fizmatlit, Moscow, 1962; Academic, New York, 1980).
10. A. Erdélyi, *Asymptotic Expansions* (Dover, New York, 1956; Fizmatgiz, Moscow, 1962).

Translated by M. Basieva